

Supporting Information

Menéndez et al. 10.1073/pnas.1009376107

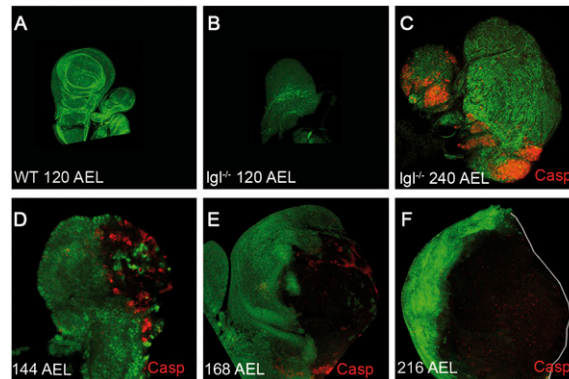


Fig. S1. Development of discs and compartments mutant for *Igl*. (A) Wild type wing disc from a 5-day-old (120 h after egg laying, AEL) late third instar larva. (B) Mutant *Igl* wing disc from a 120-h AEL larva. It is smaller than the wild type and the morphology is abnormal. (C) Fused discs from a 240-h AEL mutant larva. The morphology is aberrant and individual discs cannot be discerned. Note the regions with apoptosis, caspase activity in red. The occurrence of localized apoptosis is quite frequent, but we do not find a correlation between the amount of apoptosis and the size of the imaginal tissues, as even those showing high apoptotic levels reach a very large size. (D–F) Successive stages of growth of a wing disc in which the posterior compartment is almost entirely mutant for *Igl*. This analysis was possible because of the unexpected finding that the presence of *Igl* mutant compartments in the imaginal discs delays pupariation for a long time. Many larvae fail to pupate and continue growing until they become gigantic, very similar to homozygous *Igl* mutant larvae. It allows following the growth of the *Igl* mutant compartments well past the normal developmental time. (D) Wing disc 144 h AEL in which the posterior compartment is almost completely mutant for *Igl*. The isolated green spots are the remnants of the original *Igl*⁺ tissue in the compartment. Note the relatively small size of the posterior compartment and the high incidence of apoptosis. The P/A ratio is 0.43 ($n = 18$), whereas in the wild type, it is around 0.65. This may be due to a lower division rate of *Igl*[−] cells or to the high levels of apoptosis found in the mutant compartment. We believe the latter possibility is more likely because cell proliferation rates appear to be similar in the anterior and the posterior compartments, as indicated by BrdU incorporation. (E) Wing disc 168 h AEL of the same genotype and from the same cross as in D. There is less apoptosis than in the 144-h AEL disc but the posterior compartment is becoming bigger. The P/A ratio is now 0.84 ($n = 15$). (F) A 216-h-AEL disc of the same genotype as D and E. Notice the much bigger size of the posterior *Igl* compartment and the absence of apoptosis. Now the P/A ratio is 1.25 ($n = 10$).

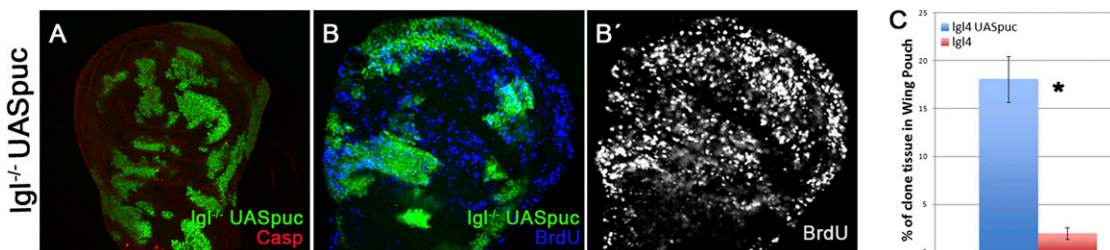


Fig. S2. Behavior of *Igl*-clones in which apoptosis is prevented by overexpressing *puc*. (A) Wing disc with several *Igl*[−] *UAS-puc* clones (green). They have normal size and shape, show no apoptosis (red), and do not produce tumors. (B and B') Disc with *Igl*[−] *UAS-puc* clones that show levels of BrdU incorporation (blue) similar to those of surrounding cells. This result suggests that *Igl* mutant cells proliferate approximately at the same rate as *Igl*⁺ cells. (C) Comparison of the areas covered by *Igl*[−] and *Igl*[−] *UAS-puc* clones in the wing pouch. The area covered by the *Igl*[−] *UAS-puc* clones is about six times bigger, indicating a strong rescue. Error bars indicate SE. * $P < 1 \times 10^{-5}$.

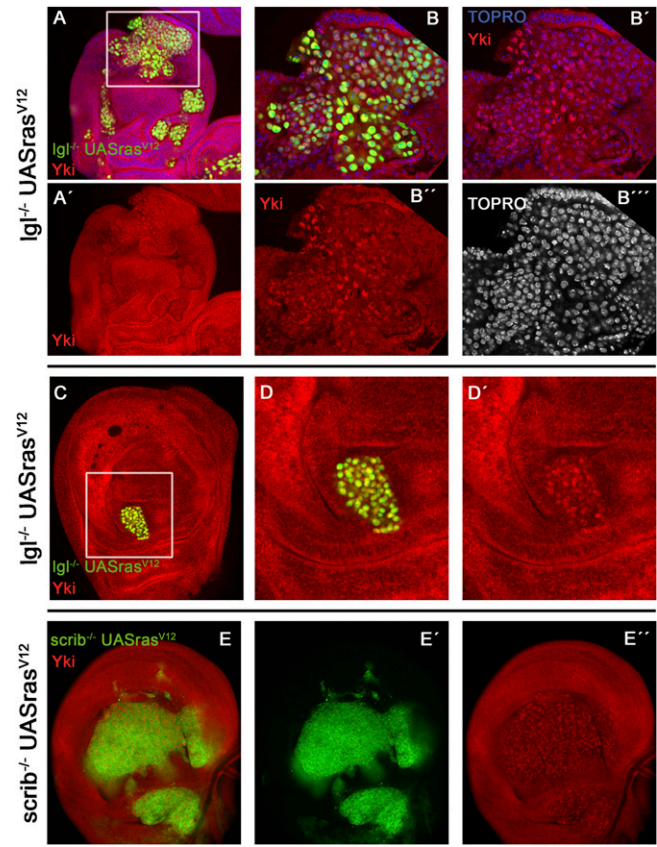


Fig. S5. Additional images showing nuclear translocation of Yki in *Igf⁻ UAS-ras^{V12}* clones and also in *scrib⁻ UAS-ras^{V12}* clones. (A and A') Disc containing several *Igf⁻ UAS-ras^{V12}* clones. Note the dotted expression of Yki (A') in the large framed clone. The clone is magnified in B-B''. Note the codistribution of nuclear GFP, TOPRO, and Yki. (C, D, and D') A small *Igf⁻ UAS-ras^{V12}* clone induced in the 7-min HS experiment also showing nuclear translocation of Yki. (E' and E'') Disc containing *scrib⁻ UAS-ras^{V12}* (cytoplasmic GFP) with nuclear localization of the Yki protein.